Theor. Comput. Fluid Dyn.
DOI 10.1007/s00162-016-0415-8

ORIGINAL ARTICLE

B. M. Shankar · I. S. Shivakumara

On the stability of natural convection in a porous vertical slab saturated with an Oldroyd-B fluid

Received: 16 April 2016 / Accepted: 1 November 2016

Abstract The stability of the conduction regime of natural convection in a porous vertical slab saturated with an Oldroyd-B fluid has been studied. A modified Darcy's law is utilized to describe the flow in a porous medium. The eigenvalue problem is solved using Chebyshev collocation method and the critical Darcy–Rayleigh number with respect to the wave number is extracted for different values of physical parameters. Despite the basic state being the same for Newtonian and Oldroyd-B fluids, it is observed that the basic flow is unstable for viscoelastic fluids—a result of contrast compared to Newtonian as well as for power-law fluids. It is found that the viscoelasticity parameters exhibit both stabilizing and destabilizing influence on the system. Increase in the value of strain retardation parameter Λ_2 portrays stabilizing influence on the system while increasing stress relaxation parameter Λ_1 displays an opposite trend. Also, the effect of increasing ratio of heat capacities is to delay the onset of instability. The results for Maxwell fluid obtained as a particular case from the present study indicate that the system is more unstable compared to Oldroyd-B fluid.

Keywords Natural convection · Vertical porous layer · Oldroyd-B fluid · Viscoelastic fluid

List of symbols

a	Vertical wave number
c	Wave speed
c_r	Phase velocity
c_i	Growth rate
$2d$	Thickness of the porous layer
$\vec{g}$	Acceleration due to gravity
$\hat{k}$	Unit vector in z-direction
K	Permeability
p	Pressure
P	Modified pressure
$\vec{q} = (u, v, w)$	Velocity vector
R_{D}	Darcy–Rayleigh number
t	Time

Communicated by Patrick Jenny.

B. M. Shankar (✉)
Department of Mathematics, PES University, Bangalore 560 085, India
E-mail: bmshankar@pes.edu

I. S. Shivakumara
Department of Mathematics, Bangalore University, Bangalore 560 056, India

Published online: 10 November 2016

T	Temperature
T_1	Temperature of the left vertical wall
T_2	Temperature of the right vertical wall
(x, y, z)	Cartesian coordinates

Greek symbols

α	Ratio of heat capacities
β	Thermal expansion coefficient
θ	Fluid temperature
Θ	Disturbance fluid temperature
λ_1	Stress relaxation time constant
λ_2	Strain retardation time constant
Λ_1	Relaxation parameter
Λ_2	Retardation parameter
μ	Fluid viscosity
κ	Effective thermal diffusivity
ρ	Fluid density
ρ_0	Reference density at T_0
ψ	Stream function
Ψ	Disturbance stream function

1 Introduction

The stability or instability of fluid flows in porous media constitutes an important part of porous media fluid mechanics. In particular, the interaction between buoyancy and shearing forces on the stability of fluid flows in a vertical layer of porous medium has been the subject of intensive research interest as many geophysical and technological phenomena are maintained by these forces. In his pioneering paper, Gill [1] investigated analytically the stability properties of natural convection in a vertical layer with reference to Darcy's flow of a Newtonian fluid with one boundary is uniformly cold while the other is uniformly hot and established that the system is always stable for all types of infinitesimal perturbations. Barletta and Alves [2] extended the analysis developed by Gill to the case of a power-law fluid and observed that the instability does not occur even for such a non-Newtonian fluid. Subsequently, many studies have been undertaken by many authors to investigate various additional effects on this problem [3–9].

As can be seen, most of the investigations are based on Newtonian fluids although many fluid dynamical systems display non-Newtonian characteristics. This has prompted researchers to consider non-Newtonian fluids which demonstrate shear-thinning, shear-thickening, viscoplastic, time-dependent (thixotropic), and viscoelastic behaviours under appropriate circumstances. For that matter, fluids often display a combination of two or even all types of the above features depending on the situations. For example, a polymer melt may show time-independent (shear-thinning) and viscoelastic behaviours simultaneously and a china clay suspension may exhibit a combination of time-independent (shear-thinning or shear-thickening) and time-dependent (thixotropic) features at certain concentrations and/or at appropriate shear rates. Thus, there exist different kinds of non-Newtonian fluids and their behaviour is different from one another. In other words, non-Newtonian fluids do not lend themselves to a unified treatment such as Newtonian fluids. Among different types of non-Newtonian fluids, viscoelastic fluids are found to be of considerable importance in various areas in science, engineering, and technology, such as material processing, petroleum, chemical, and nuclear industries, carbon dioxide geologic sequestration, bioengineering, and reservoir engineering.

The temporal development of small disturbances in magnetohydrodynamic (MHD) Jeffery–Hamel flows is investigated by Makinde and Mhone [10]. Beg and Makinde [11] addressed viscoelastic flow and species transfer in a Darcian high-permeability channel. The stability of natural convection in a vertical layer of viscoelastic liquid was first considered by Gozum and Arpaci [12], who treated the case of a Maxwell liquid while Takashima [13] investigated the problem for an Oldroyd-B liquid. Nonetheless, the flow of a viscoelastic fluid in a porous medium is an area with a multitude of applications. Obtaining oil from rocks or soil below the Earth's surface is one area which affects nearly everyone [14]. Therefore, it is pragmatic to investigate the

stability of natural convection in a vertical layer of porous medium saturated by a viscoelastic fluid which has not been reported in the open literature.

In the present study, an Oldroyd-B type of viscoelastic fluid saturating a vertical layer of Darcy porous medium is considered because the Oldroyd-B model represents adequately highly elastic (Boger) fluids for which the viscosity remains sensibly constant over a wide range of shear rates. Besides, it is one of the simplest viscoelastic laws that account for normal stress effects which are responsible for the periodic phenomena arising in viscoelastic fluids. More importantly, almost all experimental measurements and flow visualization reported on the instability of viscoelastic flow have been conducted on Boger fluids. Comparison between theory and experiment becomes possible when the Oldroyd-B constitutive equation is used. The eigenvalue problem is solved numerically using Chebyshev collocation method. The results for the Maxwellian fluid are also obtained as a particular case from the present study. Although the basic velocity remains the same for Newtonian and viscoelastic fluids, the numerical study shows that the linearly stable behaviour found by Gill [1] for Newtonian fluids does not apply for viscoelastic fluids. This paper is organized as follows. The formulation of the problem including the governing equations and the non-dimensionalization is outlined in Sect. 2. Linear stability analysis is given in Sect. 3, and the numerical method employed to solve the stability equations is described in Sect. 4. Results and discussion of the numerical solutions are given in Sect. 5. The main conclusions arrived at from this study are summarized in Sect. 6.

2 Mathematical formulation

The physical configuration of the problem is illustrated schematically in Fig. 1. We consider an Oldroyd-B fluid-saturated vertical layer of Darcy porous medium of width, $2d$. A Cartesian coordinate system (x, y, z) is chosen with the origin in the middle of the vertical porous layer, where the x-axis is taken perpendicular to the plates and the z-axis is vertically upwards, opposite to the direction of gravity $\vec{g}$. The vertical surface at $x = -d$ is impermeable and kept at a uniform temperature T_1, while the vertical impermeable surface at $x = d$ is maintained at a uniform temperature $T_2 (> T_1)$. It is well known that in the flow of viscous Newtonian fluid at a low speed through a porous medium, the pressure drop caused by the frictional drag is directly proportional to the velocity, which is the classical Darcy law. By analogy with Oldroyd-B constitutive relationships, the following phenomenological model, which relates pressure drop, body force and velocity for a viscoelastic fluid in a Darcy porous medium, is considered [14–16]:

$$\left(1 + \lambda_1 \frac{\partial}{\partial t}\right)(\nabla p - \rho \vec{g}) = -\frac{\mu}{K}\left(1 + \lambda_2 \frac{\partial}{\partial t}\right)\vec{q} \tag{1}$$

where $\vec{q} = (u, v, w)$ is the velocity vector, p is the pressure, ρ is the fluid density, μ is the viscosity of the fluid, K is the permeability, λ_1 and λ_2 are stress relaxation and strain retardation time constants, respectively. Typical fluids satisfying the Oldroyd-B constitutive relation are solutions composed of a Newtonian solvent and a polymeric solute with viscosities μ_s and μ_p, respectively. The viscosity of the solution is given by $\mu = \mu_s + \mu_p$, and hence, the ratio $\lambda_2/\lambda_1 = \mu_s/(\mu_s + \mu_p)$ is always less than or equal to unity [17,18]. We note that when λ_1 and λ_2 assume the same value, Eq. (1) is simplified to Darcy's law for the flow of viscous Newtonian fluid through a porous medium. Thus, Eq. (1) can be regarded as an approximate form of an empirical momentum equation for the flow of an Oldroyd-B fluid through a porous medium. The Oberbeck–Boussinesq approximation (since the temperature difference between the vertical plates is assumed to be small, the density is treated as a constant everywhere in the governing equation except in the gravitational term) is invoked and the model is completed by adding the continuity and energy balance equations along with the equation of state as

$$\nabla \cdot \vec{q} = 0 \tag{2}$$

$$\alpha \frac{\partial T}{\partial t} + (\vec{q} \cdot \nabla) T = \kappa \nabla^2 T \tag{3}$$

$$\rho = \rho_0 \{1 - \beta (T - T_0)\} \tag{4}$$

where T is the temperature, κ is the effective thermal diffusivity, β is the thermal expansion coefficient, ρ_0 is the density at reference temperature $T = T_0$ (at the middle of the channel), and α is the ratio of heat capacities.

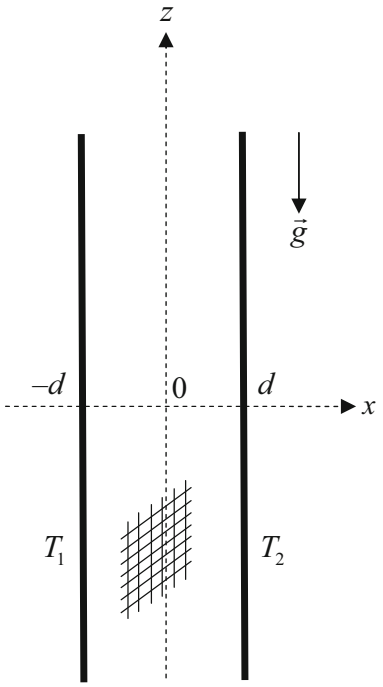

Fig. 1 Sketch of the porous channel (xz-plane section)

The quantities are made dimensionless by scaling velocity by κ/d, length by d, pressure by $\kappa\mu/K$, time by d^2/κ, and temperature by $\Delta T(=T_2-T_1)$ to get

$$\left(1+\Lambda_1\frac{\partial}{\partial t}\right)\left(\nabla P - R_{\mathrm{D}}T\hat{k}\right) = \left(1+\Lambda_2\frac{\partial}{\partial t}\right)\vec{q} \tag{5}$$

$$\alpha\frac{\partial T}{\partial t} + (\vec{q}\cdot\nabla)\,T = \nabla^2 T \tag{6}$$

where $R_{\mathrm{D}} = \rho_0 g\beta\Delta T K d/\mu\kappa$ is the Darcy–Rayleigh number, $\Lambda_1 = \lambda_1\kappa/d^2$ is the relaxation parameter, and $\Lambda_2 = \lambda_2\kappa/d^2$ is the retardation parameter. Taking curl on both sides of Eq. (5) to eliminate the modified pressure term and introducing the stream function $\psi\,(x, z, t)$ through

$$(u, 0, w) = \left(-\frac{\partial\psi}{\partial z}, 0, \frac{\partial\psi}{\partial x}\right) \tag{7}$$

the governing Eqs. (5) and (6) become

$$R_{\mathrm{D}}\left(1+\Lambda_1\frac{\partial}{\partial t}\right)\frac{\partial T}{\partial x} = \left(1+\Lambda_2\frac{\partial}{\partial t}\right)\left(\frac{\partial^2\psi}{\partial x^2}+\frac{\partial^2\psi}{\partial z^2}\right) \tag{8}$$

$$\alpha\frac{\partial T}{\partial t} + \frac{\partial\psi}{\partial x}\frac{\partial T}{\partial z} - \frac{\partial\psi}{\partial z}\frac{\partial T}{\partial x} = \frac{\partial^2 T}{\partial x^2}+\frac{\partial^2 T}{\partial z^2}. \tag{9}$$

The isothermal boundaries are impermeable, and the appropriate boundary conditions are

$$\begin{aligned}\psi &= 0, T = -1 \quad \text{at } x = -1\\ \psi &= 0, T = 1 \quad \text{at } x = 1.\end{aligned} \tag{10}$$

3 Linear stability analysis

The flow in the basic state is fully developed, unidirectional, steady, and laminar. Thus,

$$\psi = \psi_b(x), \quad T = T_b(x) \tag{11}$$

where the subscript b denotes the basic state. The basic state solution is found to be

$$\psi_b(x) = \frac{R_\mathrm{D}}{2}\left(x^2 - 1\right), \quad T_b = x \tag{12}$$

and it is same as that for an ordinary Newtonian fluid [1]. To study the linear stability of the base flow, we superimpose an infinitesimal disturbance on it in the form

$$\psi = \psi_b(x) + \psi', \quad T = T_b + T'. \tag{13}$$

Substituting Eq. (13) into Eqs. (8) and (9), and using Eq. (12), we get

$$R_\mathrm{D}\left(1 + \Lambda_1 \frac{\partial}{\partial t}\right)\frac{\partial T'}{\partial x} = \left(1 + \Lambda_2 \frac{\partial}{\partial t}\right)\left(\frac{\partial^2 \psi'}{\partial x^2} + \frac{\partial^2 \psi'}{\partial z^2}\right) \tag{14}$$

$$\alpha \frac{\partial T'}{\partial t} + R_\mathrm{D} x \frac{\partial T'}{\partial z} - \frac{\partial \psi'}{\partial z} = \frac{\partial^2 T'}{\partial x^2} + \frac{\partial^2 T'}{\partial z^2}. \tag{15}$$

Employing the normal mode analysis procedure in which we look for the solution of the form

$$\left(\psi', T'\right) = \left[\Psi(x), \Theta(x)\right] e^{ia(z-ct)} \tag{16}$$

where c is the wave speed which is real and positive and a is the vertical wave number, we then obtain

$$(1 - ia\Lambda_2 c)\left(D^2 - a^2\right)\Psi = (1 - ia\Lambda_1 c)\, R_\mathrm{D} D\Theta \tag{17}$$

$$\left(D^2 - a^2\right)\Theta + ia\Psi - ia\Theta R_\mathrm{D} x = -ia\alpha c\Theta \tag{18}$$

where $D = \partial/\partial x$.

The associated boundary conditions are:

$$\Psi = \Theta = 0 \quad \text{at } x = \pm 1. \tag{19}$$

We may now use Eq. (18) to determine Ψ in terms of Θ, and substitute it into Eq. (17), to obtain

$$\Theta'''' - 2a^2\Theta'' + a^4\Theta + iaR_\mathrm{D}\left[\left(\frac{1 - iac\Lambda_1}{1 - iac\Lambda_2}\right)\Theta' - (x\Theta)'' + a^2 x\Theta\right] = -ia\alpha c\left(\Theta'' - a^2\Theta\right) \tag{20}$$

For the Newtonian case, $\Lambda_1 = \Lambda_2$ and then Eq. (20) becomes

$$\Theta'''' - 2a^2\Theta'' + a^4\Theta + iaR_\mathrm{D}\left[a^2 x\Theta - \left(x\Theta'\right)'\right] = -ia\alpha c\left(\Theta'' - a^2\Theta\right) \tag{21}$$

which coincides with Gill [1]. Given that Ψ and Θ are complex quantities, we now multiply Eq. (20) by $\bar{\Theta}$, a complex conjugate of Θ, and integrate over the channel width. This process yields the following equation

$$\int_{-1}^{1}\left(\left|\Theta''\right|^2 + 2a^2\left|\Theta'\right|^2 + a^4\left|\Theta\right|^2\right)\mathrm{d}x + iaR_\mathrm{D}\left[\left(\frac{1 - iac\Lambda_1}{1 - iac\Lambda_2}\right)\int_{-1}^{1}\Theta'\bar{\Theta}\mathrm{d}x - \int_{-1}^{1}(x\Theta)''\,\bar{\Theta}\mathrm{d}x + a^2\int_{-1}^{1} x\left|\Theta\right|^2\mathrm{d}x\right] = ia\alpha c\int_{-1}^{1}\left(\left|\Theta'\right|^2 + a^2\left|\Theta\right|^2\right)\mathrm{d}x \tag{22}$$

Equating the real part on both sides of Eq. (22), we get

$$\int_{-1}^{1}\left(\left|\Theta''\right|^2+2a^2\left|\Theta'\right|^2+a^4\left|\Theta\right|^2\right)\mathrm{d}x+aR_{\mathrm{D}}\left(\frac{ac_r\Lambda_1-ac_r\Lambda_2}{a^2c_r^2\Lambda_2^2+(1+ac_i\Lambda_2)^2}\right)\int_{-1}^{1}\Theta'\bar{\Theta}\mathrm{d}x$$
$$=-a\alpha c_i\int_{-1}^{1}\left(\left|\Theta'\right|^2+a^2\left|\Theta\right|^2\right)\mathrm{d}x. \tag{23}$$

From Eq. (23) it is not possible to deduce the stability of the system, in general, as the value of c_i cannot be fixed. Nonetheless, for the Newtonian case ($\Lambda_1=\Lambda_2$) it is evident that c_i is always negative, and hence, the system is always stable, a result obtained for the first time by Gill [1].

4 Numerical solution

Equations (17) and (18) together with the boundary conditions (19) constitute an eigenvalue problem. This resulting eigenvalue problem is solved numerically using the Chebyshev collocation method. The kth order Chebyshev polynomial is given by

$$\xi_k(x)=\cos k\tau,\quad \tau=\cos^{-1}x. \tag{24}$$

The Chebyshev collocation points are given by

$$x_j=\cos\left(\frac{\pi j}{N}\right),\quad j=0,1,\ldots,N. \tag{25}$$

Here, the right and left wall boundaries correspond to $j=0$ and N, respectively. The field variables Ψ and θ can be approximated in terms of Chebyshev polynomials as follows

$$\Psi(x)=\sum_{j=0}^{N}\xi_j(x)\ \Psi_j,\ \Theta(x)=\sum_{j=0}^{N}\xi_j(x)\ \Theta_j. \tag{26}$$

The governing Eqs. (17)–(19) are discretized in terms of Chebyshev polynomials to get

$$(1-iac\Lambda_2)\left(\sum_{k=0}^{N}B_{jk}\Psi_k-a^2\Psi_j\right)=(1-iac\Lambda_1)\,R_{\mathrm{D}}\sum_{k=0}^{N}A_{jk}\theta_k,\ j=1\,(1)\,N-1 \tag{27}$$

$$ia\Psi_j+\left(\sum_{k=0}^{N}B_{jk}\theta_k-a^2\theta_j\right)-iaxR_{\mathrm{D}}\Theta_j=-ia\alpha c\Theta_j,\quad j=1\,(1)\,N-1 \tag{28}$$

$$\Psi_0=\Psi_N=0 \tag{29}$$

$$\Theta_0=\Theta_N=0 \tag{30}$$

where

$$A_{jk}=\begin{cases}\frac{c_j(-1)^{k+j}}{c_k(x_j-x_k)} & j\neq k\\ \frac{x_j}{2\left(1-x_j^2\right)} & 1\le j=k\le N-1\\ \frac{2N^2+1}{6} & j=k=0\\ -\frac{2N^2+1}{6} & j=k=N\end{cases} \tag{31}$$

$$\text{and } B_{jk}=A_{jm}\cdot A_{mk}. \tag{32}$$

with

$$c_j=\begin{cases}2 & j=0,\ N\\ 1 & 1\le j\le N-1.\end{cases}$$

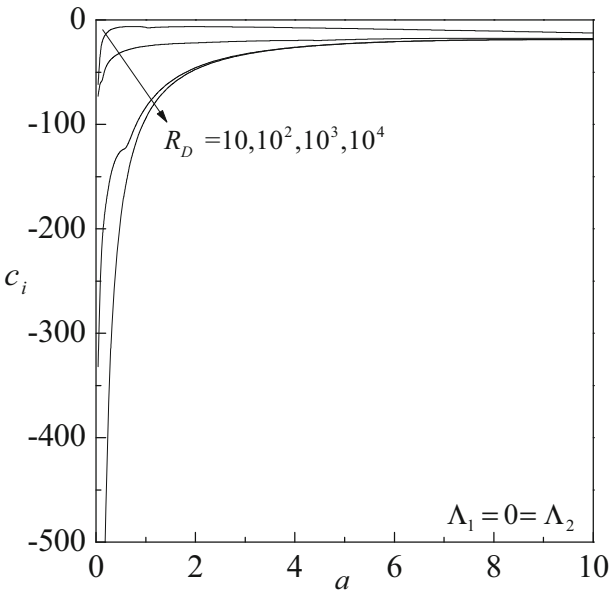

Fig. 2 Variation of growth rate c_i with wave number a for different values of R_{D} with $\Lambda_1 = 0 = \Lambda_2$ (Newtonian fluid case) when $\alpha = 1$

Equations (27)–(30) form the following system of linear algebraic equations

$$AX = cBX \tag{33}$$

where c is the eigenvalue and X is the discrete representation of the eigenfunction; A and B are square (complex) matrices of order $2(N + 1)$. By this, we mean that when one employs the time representation in ψ and T of form e^{-iact} with $c = c_r + ic_i$, then this results in ψ and T having terms of the form $e^{-iac_r t} \cdot e^{ac_i t}$. The eigenvalues are found such that the largest value of c_i is zero, and then, the result is minimized over the wave number a. The resulting R_{D} value is then the critical Darcy–Rayleigh number with corresponding wave number. The value $c_i = 0$ is chosen because this is the threshold at which the solution becomes unstable according to the linear theory. If $c_i > 0$, then ψ and T grow rapidly like $e^{ac_i t}$ and the solution is unstable.

5 Results and discussion

A classical linear stability analysis of natural convection has been performed for a vertical porous channel with impermeable and isothermal boundaries. The saturating fluid is assumed to be viscoelastic of Oldroyd-B type. The resulting generalized eigenvalue problem is solved numerically using Chebyshev collocation method. It is found that accurate solutions up to the eighth digit could be reached by taking 10 terms in the Chebyshev collocation method, and hence, the results are obtained by taking $N = 10$. The numerically computed growth rate (c_i) is exhibited in Fig. 2 as a function of wave number for $\Lambda_1 = 0 = \Lambda_2$ (Newtonian fluid case). The results show that $c_i < 0$ always for a wide range of parametric values, indicating that the system is stable. This fact is in conformity with the analytically established results of Gill [1].

The numerical computations reveal that the instability sets in always via travelling wave mode ($c_c \neq 0$) due to the elastic nature of the fluid and the related travelling wave neutral stability curves on the $(R_{\mathrm{D}}, a)-$plane for various values of Λ_1 with $\Lambda_2 = 0.2$, and Λ_2 with $\Lambda_1 = 0.2$ for a fixed value of $\alpha = 1$ are demonstrated in Fig. 3. The neutral stability curves exhibit single but different minimum with respect to the wave number for various values of these physical parameters. The region below each neutral curve corresponds to the stable state of the system. Thus, we note that increasing Λ_1 (Fig. 3a) decreases the region of stability, while opposite is the trend with increasing Λ_2 (Fig. 3b).Thus, the viscoelasticity has both stabilizing and destabilizing effects on the flow. The results shown for $\Lambda_2 = 0$ in Fig. 3b correspond to that for a Maxwell fluid.

The critical Darcy–Rayleigh number R_{Dc} corresponding to critical wave number a_c and critical wave speed c_c computed for different values of elasticity parameters are displayed in Fig. 4a–c, respectively. In

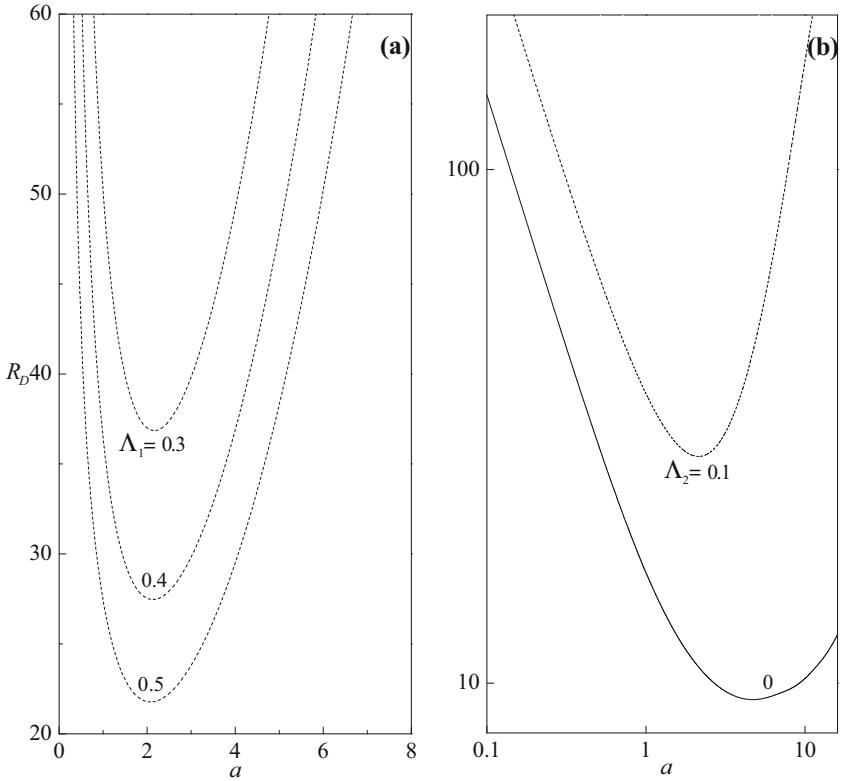

Fig. 3 Neutral stability curves for different values of **a** Λ_1 with $\Lambda_2 = 0.2$, **b** Λ_2 with $\Lambda_1 = 0.2$ when $\alpha = 1$

these figures, the curves of R_{Dc}, a_c and c_c have emanated from the value of Λ_1 exceeding the value of Λ_2. Figure 4a shows the variation of R_{Dc} as a function of Λ_1 for different values of Λ_2 when $\alpha = 1$. For higher values of Λ_2, the curves start from higher values of R_{Dc}. Henceforth, all the curves undergo a gradual fall in their values with a negative slope. For $\Lambda_2 = 0.5$, the curve experiences a steep fall in the values of R_{Dc} giving rise to a high but negative slope. Forthwith, the slope reduces (but is still negative) after $\Lambda_1 = 0.3$ and the values of R_{Dc} keep on decreasing as the curve progresses with increasing values of Λ_1. For $\Lambda_2 = 0.3$, the curve emanates from $R_{Dc} = 167$ and it experiences a similar steep decrease in R_{Dc} values till Λ_1 equals 0.2. However, in this case the duration of the negative high slope is lesser as compared to $\Lambda_2 = 0.5$ curve. Similar trend is observed for $\Lambda_2 = 0.1$ and 0.2. For $\Lambda_2 = 0$, the values of R_{Dc} keep on decreasing until Λ_1 equals 0.4 after which it almost resembles a horizontal line as the curve progresses with increasing values of Λ_1. All the curves appear parallel to the Λ_1-axis after the Λ_1 value equals 0.8. This shows that the R_{Dc} values do not show any conspicuous changes in their values compared to lower values of Λ_1 after this point. From Fig. 4a, it is also obvious that an increase in the value of strain retardation parameter Λ_2 is to increase the value of R_{Dc} and has a stabilizing effect on the system. Also, the curve of $\Lambda_2 = 0$ lies well below the curves of $\Lambda_2 \neq 0$ indicating the elasticity of a Maxwellian fluid has a more destabilizing influence on the system. The results exhibited also indicate that the effect of an increase in the stress relaxation parameter Λ_1 is to decrease R_{Dc}, and thus, it has a destabilizing effect on the flow. This may be due to the fact that the relaxation time reduces the shear rate (i.e. increases the elasticity of a viscoelastic fluid), thus causing instability.

Figure 4b establishes a relationship between a_c and Λ_1 for different values of Λ_2 when $\alpha = 1$. Only for $\Lambda_2 = 0$, the curve emerges from a very high value of a_c at 4.6. This curve then progresses forward with a slight positive increase in slope till Λ_1 equals 0.3. Forthwith, the curve resembles a horizontal line with a minute change in a_c with an increase in Λ_1 value. For all the other values of Λ_2, the curves emanate from a common origin point at $a_c = 2.188$. However, the progression of each curve is very different as the value of Λ_1 increases. The curve for $\Lambda_2 = 0.5$ is a straight horizontal line parallel to the Λ_2-axis. This shows that the values of a_c when $\Lambda_2 = 0.5$ remain constant irrespective of the value of Λ_1. However, the curve for $\Lambda_2 = 0.3$ display slight variations. The curve progresses with a constant value in a_c till Λ_1 equals 0.4. Forthwith, the values of a_c begin to decrease gradually as the curve progresses with increasing values of Λ_1. For $\Lambda_2 = 0.2$, the

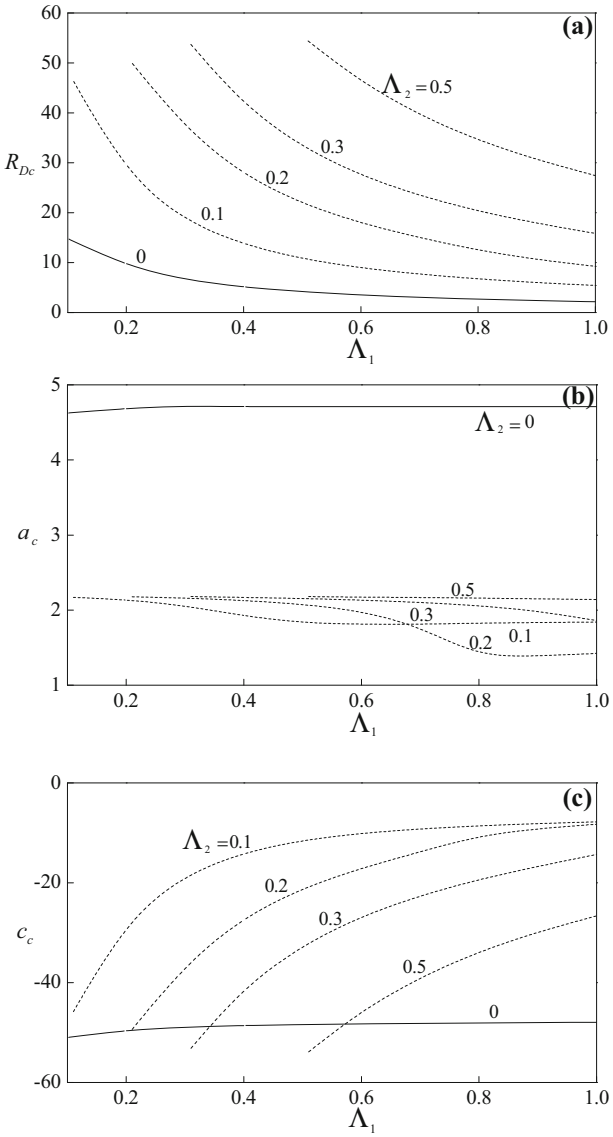

Fig. 4 Variation of **a** R_{Dc}, **b** a_c, and **c** c_c with Λ_1 for various values of Λ_2 when $\alpha = 1$

curve the horizontal and has the same values of a_c as curves for $\Lambda_2 = 0.5, 0.3$ until Λ_1 equals 0.3. Thereafter the curves experience digression and the curve for $\Lambda_2 = 0.2$ experiences a gradual fall in a_c values as the values of Λ_1 increase. However, once Λ_1 equals 0.6, the values of a_c fall sharply with the curve developing a highly negative slope. $\Lambda_1 = 0.8$ is an inflection point where there is a change in the curve and after that point the slope starts to slightly increase towards the positive side. The curve for $\Lambda_2 = 0.1$ has a slightly negative slope at the beginning until Λ_1 equals 0.45. Till this point, the values of a_c keep reducing for increasing values of Λ_1. However, after this point there is a gradual increase in the values of a_c till the curve almost becomes a straight line with constant values of a_c approximately. The curves of $\Lambda_2 = 0.3$ and 0.1 intersect at $a_c = 1$, and this shows that both the curves have the same start point and end point even if their path was very different.

The curves of critical wave speed c_c displayed in Fig. 4c as a function of Λ_1 for different values of Λ_2 indicate that the instability sets in via travelling wave mode. It is seen that the curve of c_c for a Maxwell fluid ($\Lambda_2 = 0$) is independent on the values of Λ_1 while the curves of c_c for other values of $\Lambda_2 \neq 0$ remain almost constant and come together with increasing Λ_1. It is also evident that Λ_1 and Λ_2 exhibit opposite effects on c_c.

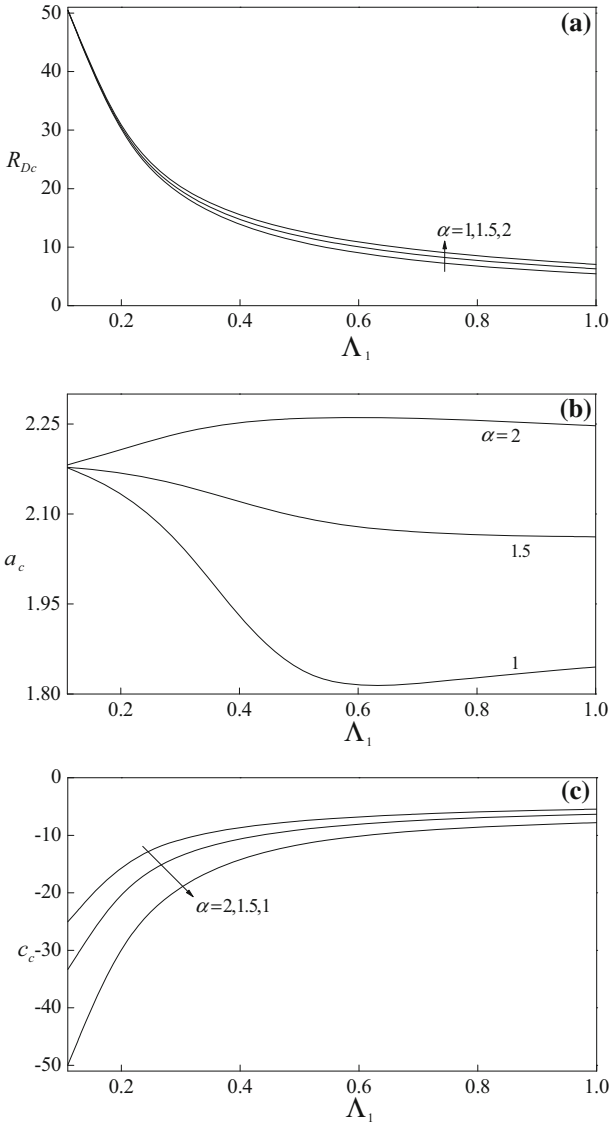

Fig. 5 Variation of **a** R_{Dc}, **b** a_c, and **c** c_c with Λ_1 for various values of α when $\Lambda_2 = 0.1$

Figure 5a, b illustrates R_{Dc} and a_c as a function of Λ_1, respectively, for different values of $\alpha = 1, 1.5, 2$ when $\Lambda_2 = 0.1$. It is evident that all the three curves follow a similar trend. They emanate from $R_{\mathrm{Dc}} = 50.4$ and forthwith experience an exponential decline in their values. The curves progress identically till the value of $\Lambda_1 = 0.2$ after which the gradient reduces significantly and the curves diverge. All the three curves experience a steady decline in R_{Dc} with increasing Λ_1. From Fig. 5a, it is clear that increase in the value of α leads to increase in the value of R_{Dc}, and thus, it has a stabilizing effect on the system. This may be due to decrease in the value of heat capacity of the fluid. The curves of critical wave number emerge from $a_c = 2.17$ for all the values of α as shown in Fig. 5b and note that increase in α is to increase a_c considerably. Thus, the effect of increasing α is to contract the size of convection cells. Figure 5c shows that increasing α is to increase the critical wave speed.

6 Conclusions

The stability of natural convection in a vertical layer of an Oldroyd-B fluid-saturated Darcy porous medium whose vertical walls are impermeable and kept at different uniform temperatures has been investigated. The

governing dimensionless parameters are the Darcy–Rayleigh number, R_D, relaxation parameter, Λ_1, retardation parameter, Λ_2, and the ratio of heat capacities α. In contrast to the Newtonian and power-law fluids, the system becomes unstable via travelling wave mode in the case of viscoelastic fluids. The influence of Λ_1 and Λ_2 on the stability of the system is opposite in nature and they display destabilizing and stabilizing effects on the system, respectively. Depending on the parametric values, there exist threshold values of Λ_1 and Λ_2, above and below which the flow becomes unstable, respectively. The effect of increasing ratio of heat capacities has a stabilizing effect on the system. The results for the Maxwell fluid exhibit that the system is more unstable compared to Oldroyd-B type of viscoelastic fluids. Moreover, the critical wave numbers for Maxwell fluid are higher than those of Oldroyd-B fluid.

Acknowledgements The authors acknowledge with thanks Prof. D.A.S. Rees for providing the translated (Russian to English) version of the paper of Alishaev and Mirzadjanzade [15]. We thank the anonymous referees for their constructive comments, which helped us to improve the manuscript. One of the authors B.M.S wishes to thank the authorities of his University for the encouragement and support.

References

1. Gill, A.E.: A proof that convection in a porous vertical slab is stable. J. Fluid Mech. **35**, 545–547 (1969)
2. Barletta, A., Alves, L.S.B.: On Gill's stability problem for non-Newtonian Darcy's flow. Int. J. Heat Mass Transf. **79**, 759–768 (2014)
3. Rees, D.A.S.: The stability of Prandtl–Darcy convection in a vertical porous slot. Int. J. Heat Mass Transf. **31**, 1529–1534 (1988)
4. Lewis, S., Bassom, A.P., Rees, D.A.S.: The stability of vertical thermal boundary layer flow in a porous medium. Eur. J. Mech. B **14**, 395–408 (1995)
5. Kwok, L.P., Chen, C.F.: Stability of thermal convection in a vertical porous layer. ASME J. Heat Transf. **109**, 889–893 (1987)
6. Qin, Y., Kaloni, P.N.: A nonlinear stability problem of convection in a porous vertical slab. Phys. Fluids A **5**, 2067–2069 (1993)
7. Rees, D.A.S.: The effect of local thermal nonequilibrium on the stability of convection in a vertical porous channel. Transp. Porous Med. **87**, 459–464 (2011)
8. Shankar, B.M., Kumar, J., Shivakumara, I.S.: Stability of natural convection in a vertical couple stress fluid layer. Int. J. Heat Mass Transf. **78**, 447–459 (2014)
9. Shankar, B.M., Kumar, J., Shivakumara, I.S.: Effect of horizontal alternating current electric field on the stability of natural convection in a dielectric fluid saturated vertical porous layer. J. Heat Transf. **137**, 042501 (2015)
10. Makinde, O.D., Mhone, P.Y.: Temporal stability of small disturbances in MHD Jeffery–Hamel flows. Comput. Math. Appl. **53**, 128–136 (2007)
11. Beg, O.A., Makinde, O.D.: Viscoelastic flow and species transfer in a Darcian high-permeability channel. J. Petrol. Sci. Eng. **76**, 93–99 (2011)
12. Gozum, D., Arpaci, V.S.: Natural convection of viscoelastic fluids in a vertical slot. J. Fluid Mech. **64**, 439–448 (1974)
13. Takashima, M.: The stability of natural convection in a vertical layer of viscoelastic liquid. Fluid Dyn. Res. **11**, 139–152 (1993)
14. Straughan, B.: Stability and Wave Motion in Porous Media. Springer, New York (2008)
15. Alishaev, M.G., Mirzadjanzade, AKh: For the calculation of delay phenomenon in filtration theory. Izvestya Vuzov, Neft I Gaz **6**, 71–78 (1975)
16. Khuzhayorov, B., Auriault, J.L., Royer, P.: Derivation of macroscopic filtration law for transient linear viscoelastic fluid flow in porous media. Int. J. Eng. Sci. **38**, 487–504 (2000)
17. Bird, R.B., Stewart, W.E., Lightfoot, E.N.: Transport Phenomena. Wiley, Hoboken (2007)
18. Hirata, S.C., de Alves, L.S.B., Delenda, N., Ouarzazi, M.N.: Convective and absolute instabilities in Rayleigh-Bénard-Poiseuille mixed convection for viscoelastic fluids. J. Fluid Mech. **765**, 167–210 (2015)